https://doi.org/10.1016/j.ijhydene.2022.06.007

Laminar flame speed correlations of ammonia/hydrogen mixtures at high pressure and temperature for combustion modeling applications

V. Pessina[a)], F. Berni[a)], S. Fontanesi[a)], A. Stagni[b)], M. Mehl[b)],

[a)] *University of Modena and Reggio Emilia, Department of Engineering "Enzo Ferrari", Via Vivarelli 10, Modena 41125, Italy*

[b)] *Department of Chemistry, Materials, and Chemical Engineering "G. Natta", Politecnico di Milano, 20133 Milano, Italy*

Abstract. Ammonia/hydrogen mixtures are among the most promising solutions to decarbonize the transportation and energy sector. The implementation of these alternative energy carriers in practical systems requires developing suitable numerical tools, able to estimate their burning velocities as a function of both thermodynamic conditions and mixture quality. In this study, laminar flame speed correlations for ammonia/hydrogen/air mixtures are provided for high pressures (40 bar to 130 bar) and elevated temperatures (720 K to 1200 K), and equivalence ratios ranging from 0.4 to 1.5. Based on an extensive dataset of chemical kinetics simulations for ammonia/hydrogen blends (0-20-40-60-80-90-100 mol% of hydrogen), dedicated correlations are derived using a regression fitting. Besides these blend-specific correlations, a generalized (i.e., hydrogen-content adaptive) formulation, with hydrogen content used as additional parameter, is proposed and compared to the dedicated correlations.

Keywords: ammonia/hydrogen mixtures, chemical kinetics, laminar flame speed correlations, flamelet combustion modelling

Highlights:

- Ammonia/air mixtures with increasing hydrogen content for wide range of conditions
- Chemical kinetics simulations are performed at high pressures and temperatures
- Blend-specific correlations are developed for combustion CFD codes
- A generalized and hydrogen-content adaptive correlation is derived
- Limited prediction error and satisfying comparison with state-of-art is achieved

1. Introduction

The wide-spreading concerns about climate change are pushing policymakers and the scientific community to find alternative solutions to traditional power generation technologies, enhancing the efficiency of processes and the sustainability of sources. Nowadays, combustion is the main process used for power generation in both (road and marine) transportation and energy production (e.g. power plants or stationary power generation) and, because of its many technological advantages, it is expected to remain a major player for most of the 21st century [1]. In the pursuit of the decarbonization, processes involving combustion must convert to carbon-neutral fuel sources and energy carriers. In this context, hydrogen (H_2) and ammonia (NH_3) are regarded with interest, as they can be applied in internal combustion engines (ICEs), gas turbine burners [2], as well as furnaces[3][4][5], and their oxidation is characterized by the absence of carbon-based pollutants, such as CO, CO_2, and soot. NH_3 can be conveniently stored as a liquid (at 8 bar and 21 °C) and it has higher energy density when compared to liquid H_2, thus it is a suitable energy carrier for H_2 as reported by [4] [6]. However, their combustion process needs to be thoroughly controlled to mitigate the formation of other pollutant species, e.g., Nitrogen Oxides (NO_x). Lee et al. [7] published an experimental and computational study regarding NH_3 blending in H_2 /air spark-ignited spherical flames evaluating the effect of NH_3 addition on both emissions and flame behavior. For lean conditions, the addition of NH_3 increases the production of NO_x compared to H_2 /air flames, whereas for richer mixtures the production of NO_x is reduced [7]. A thorough review on NO_x formation stemming from ammonia use in combustion device was presented by [5]. The flame behavior and NO_x production were also extensively studied by Karan [8], Hayakawa [9], and by Mashruk et al. [10]. The interplay of thermal decomposition, residence time, and heat losses in NO_x formation was also investigated by Okafor[11] with highlights on combustor wall and flame interactions. Interestingly, NH_3 provides a potential suppression effect of preferential-diffusional and hydrodynamic instabilities which characterize ultra-lean and lean H_2 /air mixtures; particularly, in this regard, NH_3 appears more effective than methane, one of the most employed H_2 -carriers. Despite its stabilization effect on H_2 /air lean flames, the use of NH_3 must be carefully investigated considering

its potential high reactivity with the container materials and its toxicity[6]. NH_3 and H_2 blends for power generation have been extensively investigated by the scientific community, with studies ranging from experimental characterization to computational modelling, from gas turbine applications [12] to spark ignition engines [13]. Experiments are essential to characterize the combustion behavior of NH_3 mixtures: they provide information to derive and validate reaction mechanisms, which are employed in chemical kinetics simulations to calculate ignition delays, laminar flame speeds, and pollutant formation. The study presented by Shrestha et al. [14] includes both experimental and modelling approaches for the derivation of chemical kinetics models for the oxidation of NH_3/H_2 blends at high temperatures, as well as those carried out by [8] and at conditions representative of commercial micro-turbines [15]. Chemical kinetics can be either directly integrated in CFD solvers via the solution of transport equation for reactants and products, or used off-line, to create libraries where ignition delays, laminar flame speeds or species formation are stored as function of thermodynamic parameters and mixture quality. Such libraries can be employed in association with specific models in the CFD solver to retain high fidelity in the chemical characterization of the mixture while reducing the overall computational cost of the simulations. Regardless of the approach, the integration of detailed chemical kinetics in the CFD process provides further insight on the combustion behavior within a specific device, and this is particularly true for unconventional fuels, such as NH_3. The use of NH_3 as an energy carrier was extensively discussed by [3], [4], [12]. Xiao et al. [12] applied CFD to a gas turbine burner fueled with NH_3/CH_4 /air mixtures, whereas for internal combustion engines applications, NH_3 blends have already been the subject of experimental studies, as the one conducted by Lhuillier et al.[16], Verhelst et al. [17], and Chiong et al. [13] carried out a study regarding ammonia fueled engines.

As for numerical modelling of premixed or partially premixed turbulent combustion in ICEs, which mostly falls in the wrinkled-flamelet regime[18] [19], the accurate description of flame propagation is based on a proper characterization of the laminar burning velocity of the mixture and on a correct representation of turbulent acceleration of the laminar-like flame via correlations [20]. The CFD solver employ as input the laminar flame speed correlations to compute the turbulent flame propagation, treating the turbulent combustion as a laminar flame with an increased flame surface area. For this reason, reliable laminar flame speed correlations are essential to achieve a correct modelling of turbulent combustion, which is the predominant one in industrial applications.

The laminar burning velocity of a mixture is the result of its composition, as well as its temperature and pressure, and summarizes into a single value the effects of chemical kinetics, thermodynamics, and diffusion [21]. The stark differences in the combustion behavior between H_2 , NH_3 and hydrocarbons (e.g., alkanes, such as CH_4) require dedicated modelling of the flame propagation, thus a laminar flame speed description tailored on specific fuel composition is essential to achieve sufficient accuracy when modelling the combustion process. Traditionally, laminar flame speed correlations are derived using a fitting procedure of available experiments [22] [23] [24]. While they provide high accuracy at conditions close to the experimental ones, the validity of their extrapolation outside that range is not guaranteed. Experimental studies are available [14] [25] [26] [27] [28] [29] at several conditions, though still far from the targeted ICE ones (i.e., for pressures ranging from 40 bar to 130 bar). Alternatively, chemical kinetics simulations can be carried out at engine-like conditions to provide a dataset of virtual experiments to formulate correlations suitable for full-load engine conditions. Several reaction mechanisms for chemical kinetics applications are available: an NH_3/H_2 /air reaction mechanism (26 species and 119 reactions) was proposed by Gotama et al [30] by working on the optimization of the mechanism presented by Han et al.[31] and perfecting the lean and rich conditions; a study that comprises of CH_4 /NH_3 mixtures was presented by Okafor et al. [32], whereas an alternative reaction mechanism was proposed by Otomo et al. [33] on chemical kinetics of NH_3/H_2 /air mixtures with focus on laminar flame speed. Finally, a detailed kinetic mechanism was proposed by Stagni et al. [34] [35]. As for the laminar flame speed correlations, extensive research has been done for hydrocarbon-based fuels [36] and gasoline surrogates [37] [38]. In the wake of the current focus on decarbonization, new studies on carbon-neutral and unconventional fuels, such as NH_3 and H_2 , have emerged. An extensive study on H_2 laminar flame speed was proposed by Verhelst et al. [39] [40], in which correlations for H_2 /air mixtures at engine relevant conditions (pressures up to 45 bar) were presented. Another correlation based on chemical kinetics simulations for pure H_2 was proposed by D'Errico et al. [41]. This correlation covers pressures up to 16 bar, and it was tested in one-dimensional thermo-fluid dynamic simulations of a S.I. engine. Goldmann et al. [42] successfully derived laminar flame speed correlations for mixtures of NH_3 (0–100 mol%)-H_2 (0–60mol%)-air, for 1 bar $\leq p \leq$ 250 bar, $0.5 \leq \lambda \leq 1.7$, 300 K $\leq T_u \leq$ 1000 K (where the air index λ is equal to the inverse of the equivalence

ratio Φ, $\lambda = \Phi^{-1}$). Despite these previous works, in the authors' view, the existing literature lacks correlations for typical ICE full-load conditions. This work aims to fill this gap.

The present study addresses the issue of the availability of correlations for NH_3/air mixtures with increasing H_2 content, at typical full-load engine conditions (40 bar $\leq p \leq$ 130 bar) and from ultra-lean to rich mixtures ($0.4 \leq \Phi \leq 1.5$). In particular, laminar flame speed correlations are derived for NH_3/air mixtures with an increasing H_2 percentage (0-20-40-60-80-90-100 mol%) using a fitting procedure on an extensive dataset of chemical kinetics simulations. Finally, a single laminar flame speed correlation accounting for H_2 mole fraction as an additional independent parameter is presented for lean-to-rich conditions ($0.7 \leq \Phi \leq 1.5$) for NH_3/air mixtures with high H_2 contents (60-80-90 mol%), and its effectiveness is compared to the results obtained with blend-specific correlations from dedicated fitting procedures.

2. Methodology

2.1 Laminar flame speed database and chemical kinetics

In the present study, laminar flame speed prediction via fitting of chemical kinetics simulations is proposed using DARS v4.30, licensed by Siemens PLM. Freely propagating laminar flames are simulated in a one-dimensional reactor using reaction mechanisms, thermodynamics, and transport data developed by Stagni et al. [35]. Although its validation is documented in [35], a comparison with the reaction mechanisms proposed by Shrestha [14], Gotama [30], and Otomo [33] is proposed for NH100 (100 mol% of NH_3) and NH80 (80 mol% of NH_3) in **Fig. 1(a)** and **Fig. 1(b)** respectively. Simulation outcomes are reported for freely propagating laminar flames at 450 K and 1 bar. Given its fundamental role in the combustion reaction mechanisms of hydrocarbons, H_2 chemical kinetics has been extensively studied, whereas the combustion reactions of NH_3 came under scrutiny only more recently. NH_3 mechanisms present higher uncertainties and variability, therefore the comparison between reaction mechanisms is carried out for blends in which the NH_3 oxidation chemistry is predominant.

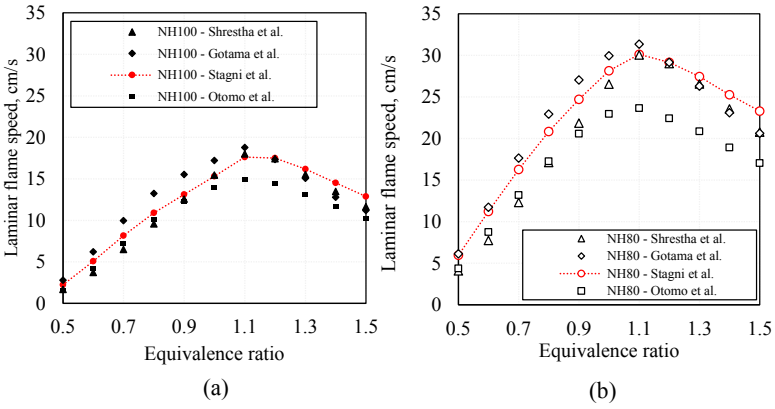

Figure 1. Results with different reaction mechanisms at 450 K and 1 bar for NH100 (a) and NH80 (b).

2.2 Dedicated fitting for NH_3/H_2 /air mixtures

The fitting procedure adopted in this work was firstly proposed by Brusca et al. [43], further developed by the authors, and successfully employed for hydrocarbon-based fuels [36] [37]. In the first part of this study, this procedure is applied to carbon-neutral fuels mixtures of H_2 and NH_3 for the derivation of dedicated laminar flame speed correlations. The foundational database used includes laminar flame speed values from chemical kinetics simulations at engine-like conditions, (**Table 1)**, for different NH_3/air, H_2 /air and NH_3/H_2 /air mixtures (**Table 2**).

p (bar)	$T_{u,\,low}$ (K)	$T_{u,\,med}$ (K)	$T_{u,\,high}$ (K)
40	720	820	920
50	752	852	952
60	784	884	984
70	816	916	1016
80	848	948	1048
90	880	980	1080
100	912	1012	1112
110	944	1044	1144
120	976	1076	1176

130	1008	1108	1208

Table 1. Engine conditions.

Blend	NH100	NH80	NH60	NH40	NH20	NH10	NH0
NH_3 mol%	100	80	60	40	20	10	0
H_2 mol%	0	20	40	60	80	90	100

Table 2. NH_3/H_2 blends investigated in this study.

The laminar flame speed is expressed as function of pressure, unburnt temperature, and equivalence ratio, as reported in **Eq. 1**.

$$s_L = s_L(p, T_u, \Phi) \tag{1}$$

The fitting procedure is applied to more than 2500 simulated laminar flame speed values (360 for each blend) and exploits two distinct functions depending on the equivalence ratio Φ range to minimize the fitting errors. A fitting procedure for lean to rich mixtures ($0.7 \leq \Phi \leq 1.5$) results in coefficients reported in **Table 3** for the calculation of the laminar burning velocity via **Eq. 2**:

$$s_L(\Phi) = \sum_{i=0}^{5} a_i \cdot (\ln(\Phi))^i \cdot \left(\frac{T_u}{T_0}\right)^{\sum_{i=0}^{5} b_i \cdot (\ln(\Phi))^i} \cdot \left(\frac{p}{p_0}\right)^{\sum_{i=0}^{5} c_i \cdot (\ln(\Phi))^i} \tag{2}$$

The poly-logarithmic expression (**Eq. 2**) can successfully represent the bell-shaped data trend from lean to rich conditions. However, the use of this procedure for an extended range of equivalence ratio values (that comprises also of the ultra-lean conditions) would result in increased prediction errors [36]. A different polynomial expression that operates a linear scaling on the pressure and temperature conditions can reduce the error in the ultra-lean range as extensively discussed in [36] [37]. Thus, ultra-lean conditions ($0.4 \leq \Phi < 0.7$) are treated using a dedicated fitting methodology: pressure and temperature scaling factors are derived and employed in the laminar flame speed calculation. Although the functions and the data-fitting techniques differ, the continuity of the polynomial expression is

ensured by linking the laminar flame speed value of the lower limit (Φ = 0.7) of **Eq. 2** to the upper limit of the ultra-lean branch of the laminar burning velocity **Eq. 3** [36]. This scaling procedure was successfully applied to laminar flame speeds for hydrocarbon-based fuels at engine-like conditions [36] and its effectiveness is tested in this study for NH_3 and H_2 fuels. The final value of the laminar burning velocity for ultra-lean mixtures is obtained by weighting pressure and temperature scaling factors (PSF and TSF respectively) as shown in **Eq. 3**, where $s_L(\Phi|_{0.7}, T_u)$ is the burning velocity value at $\Phi = 0.7$ calculated using **Eq.2**, w_p and w_T are the weights for pressure and temperature scaling respectively, and PSF and TSF are calculated via **Eq .4** and **Eqs. 5, 6** and **7**, respectively. Equations for ultra-lean laminar flame speed predictions are shown for the lowest temperature level, but they are valid for high and medium temperature levels [36] as well, using the respective coefficients reported in the results section.

$$s_L(\Phi, T_u) = s_L(\Phi|_{0.7}, T_u) \cdot \frac{(PSF(\Phi)\cdot w_p + TFS_{low}(\Phi, T_u)\cdot w_T)}{(w_p + w_T)} \quad (3)$$

$$PSF(\Phi) = \frac{l_3|\Phi - 0.7|^3 + l_2|\Phi - 0.7|^2 + l_1|\Phi - 0.7| + l_0}{l_0} \cdot \left[1 + m_2 \cdot \frac{p - p_{ref}}{p_{ref}} \cdot \frac{|\Phi - 0.7|}{|0.7 - 0.4|}\right] \quad (4)$$

$$TFS_{low}(\Phi, T_u) = m_{low}(\Phi) \cdot \frac{T_u}{T_{ref}} + q_{low}(\Phi) \quad (5)$$

$$m_{low}(\Phi) = ml_2^{low} \cdot (\Phi)^2 + ml_1^{low} \cdot (\Phi) + ml_0^{low} \quad (6)$$

$$q_{low}(\Phi) = ql_2^{low} \cdot (\Phi)^2 + ql_1^{low} \cdot (\Phi) + ql_0^{low} \quad (7)$$

2.3 Generalized correlation for increasing H_2 content in NH_3/air blends

NH_3 is characterized by slow laminar burning velocities, especially if compared to H_2. When blended with H_2, the laminar flame speed of NH_3/air mixtures considerably increases. The acceleration of the laminar flame speed with the increase of H_2 is related to the H_2-chemistry chain branching reaction $O_2 + H = OH + O$, which is the most sensitive reaction for NH_3 as well. This reaction sensitivity grows with the increment of H_2, thus the laminar burning velocity accelerates [6]. While blends with scaled levels of dilution (e.g. Exhaust Recirculation Gas EGR) show a linear blending behavior, relatively small amounts of NH_3 have a stronger than expected inhibiting effect on flame propagation. In detail, as visible in **Fig. 2**, the trend of the laminar burning velocity increment with H_2 addition is exponential:

the enhancement is limited for low H_2 content, while the growth rate becomes progressively steeper for higher concentrations, and this is partially due to the increased relevance of the H_2 -chemistry chain branching reaction [6] and to its relatively high reactivity [25]. A similar behavior is reported by Di Sarli et al. [44] and by Mitu et al. [29] for H_2 /CH_4 /air mixtures.

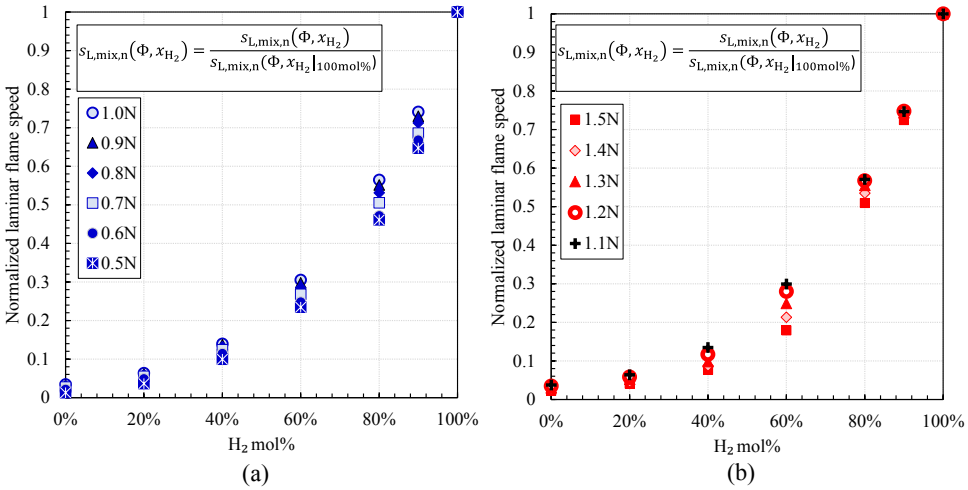

Figure 2. Laminar flame speed values at 400 K and 1 bar for increasing H_2 content (from 0mol% to 100mol%), for ultra-lean to stoichiometric (a) and for rich (b) mixtures.

The impact of H_2 addition depends on the properties of the other component(s) of the fuel mixture. An example is depicted in **Fig. 3**: for stoichiometric, lean, and rich mixtures the impact of increasing level of H_2 on laminar burning velocity is shown for fuels characterized by different molecular weight, such as iso-octane (114 g/mol), ethane (30 g/mol), methane (16 g/mol), and NH_3 (17 g/mol). The relative increment $\Delta s_L(\bar{\Phi}, x_{H_2})$ is the difference of the laminar flame speed values of blend $s_L(\bar{\Phi}, x_{H_2})$ and the pure component $s_L(\bar{\Phi}, x_{H_2}|_{0mol\%})$, normalized over the latter: $\Delta s_L(\bar{\Phi}, x_{H_2}) = [s_L(\bar{\Phi}, x_{H_2}) - s_L(\bar{\Phi}, x_{H_2}|_{0mol\%})]/s_L(\bar{\Phi}, x_{H_2}|_{0mol\%})$. Since iso-octane and methane are not available in the mechanism adopted in this study [35], the results presented in **Fig. 3** stem from chemical kinetics simulations using the reaction mechanism proposed by CRECK Modeling Group [45] [46] [47]. As shown in **Fig. 3**, the increase of laminar flame speed due to H_2 addition is relevant at very high values of H_2 mole fraction x_{H_2}, especially for the heavier compounds, such as iso-octane: the heavier the hydrocarbon the lower the mass fraction of H_2 in the mixture, for a fixed value of the mole fraction. As a reference for **Fig. 3**, values of the laminar flame speed for fuel without H_2 addition are listed for

the stoichiometric combustion: 60 cm/s methane, 71 cm/s ethane, and 57 cm/s iso-octane, whereas 12 cm/s ammonia for a test point characterized by 400 K and 1 bar. This suggests that, in case large discrepancies exist among the molecular weights of the individual components, the adoption of mole fraction-based mixing rules may be biased towards the lighter ones. This is confirmed by the analysis of C_8H_{18}/H_2 mixtures, where a marked speed-up of laminar flame speed can be spotted only for very high x_{H_2} (~ 90-95%), corresponding to ~ 10-15% mass fraction. Despite all fuels show consistent trends, a general correlation between laminar flame speed increase and molecular weight ratio cannot be established: interestingly, the increase in laminar burning velocity is more significant for NH_3, than for CH_4, despite their very similar molecular weights.

In the light of the observations above, a generalized description of the laminar flame speed with H_2 content as an additional parameter $s_L = s_L(p, T_u, \Phi, x_{H_2})$ can be achieved using an exponential law, that increases the velocity with the increment of the H_2 mole fraction x_{H_2}.

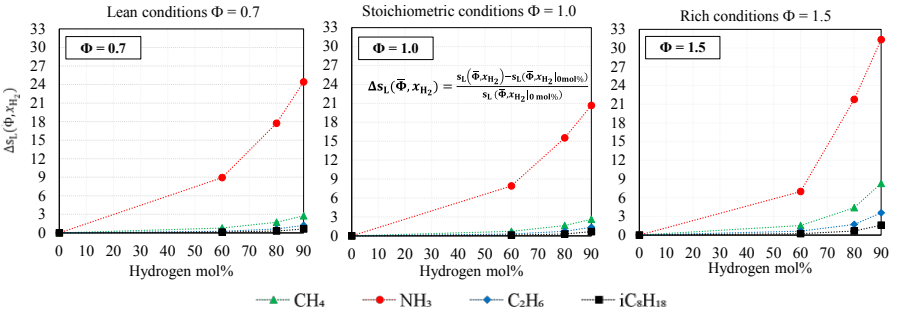

Figure 3. Relative increment of laminar flame speed with increasing H_2 content (chemical kinetics simulations at 400 K and 1 bar).

The correlation proposed in this study is valid for NH_3/air blends with an additional H_2 content ranging from 60 mol% to 90 mol% and for ($0.7 \leq \Phi \leq 1.5$) and for thermodynamic conditions reported in **Table 1**. It is based on a scaling function parametrized on equivalence ratio and H_2 mole fraction (x_{H_2}), as reported in **Eq. 8**. Such function scales the pure H_2 laminar flame speed depending on the blend composition. The scaling factor $A(\Phi)$ and the exponential factor $a(\Phi)$ are computed using data related to NH40 (60mol% of H_2), NH20 (80mol% of H_2), and NH10(90mol% of H_2) chemical kinetics simulations. Firstly, for a fixed equivalence ratio $\bar{\Phi}$, laminar flame speeds $s_{L,mix}(\bar{\Phi}, x_{H_2})$ are normalized

considering the corresponding value $s_{L,H_2}(\bar{\Phi})$ of the pure H_2 /air mixture (NH0). Values of $A(\bar{\Phi})$ and $a(\bar{\Phi})$ for each fixed equivalence ratio value are derived from a fitting procedure using an exponential expression, as reported in **Eq. 8**. The variation of $A(\Phi)$ and $a(\Phi)$ with the equivalence ratio is then analyzed: as visible in **Fig. 4**, a quasi-linear trend can be observed, thus their value can be described as a linear polynomial expression as reported in **Eqs. 9** and **10** respectively. It is important to point out that the value of the H_2 laminar flame speed in **Eq. 8** is calculated using the polynomial expression in **Eq. 2** and not from the chemical kinetics simulations results.

$$s_{L,mix}(\Phi, x_{H_2}) = s_{L,H_2}(\Phi) \cdot A(\Phi) \cdot e^{[a(\Phi) \cdot x_{H_2}]} \quad (8)$$

$$a(\Phi) = am \cdot \Phi + qa \quad (9) \qquad A(\Phi) = Am \cdot \phi + Aq \quad (10)$$

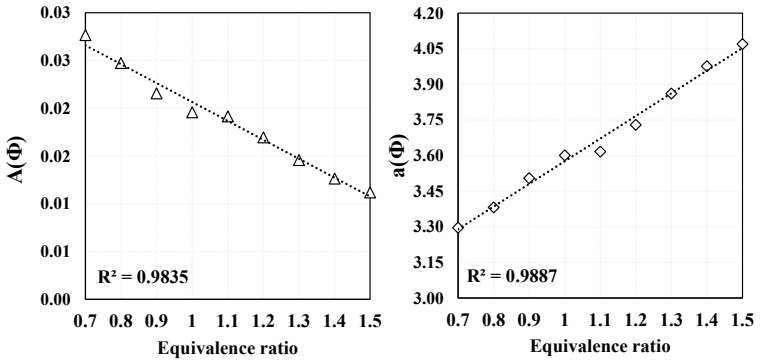

Figure 4. Linear trend of the scaling and exponential factor for lean to rich conditions.

3. Results and Discussion

3.1 Laminar flame speed prediction

A summary of the equations and coefficients produced with the fitting procedure discussed in the methodology section is reported here:

- lean-to-rich conditions ($0.7 \leq \Phi \leq 1.5$) coefficients in **Table 3** for **Eq. 2**.
- ultra-lean mixtures ($0.4 \leq \Phi < 0.7$) coefficients in **Table 4** for **Eqs. 3**, **4**, **5**, **6** and **7**.

- H_2 -scaled correlation for 60 mol% $\leq x_{H2} \leq$ 90 mol% and for $0.7 \leq \Phi \leq 1.5$, expressed via **Eqs. 8**, **9** and **10** whose coefficients are proposed in **Table 5**.

lean - stoichiometric - rich mixtures $0.7 \leq \Phi \leq 1.5$							
	NH100	NH80	NH60	NH40	NH20	NH10	NH0
a_0	40.01732323	57.52264	87.45705	147.5105	291.8279	464.277	858.1271
a_1	53.57696535	72.47356	109.5226	186.1306	425.1703	724.4504	1455.061
a_2	-35.99989985	-50.3331	-67.7463	-117.413	-143.923	-134.024	40.84949
a_3	-488.7584133	-580.496	-752.652	-1025.55	-1728.01	-2116.31	-2092.01
a_4	-211.165836	-237.118	-306.023	-335.115	-723.676	-934.813	-827.723
a_5	1901.521526	2225.961	2830.463	3550.917	5158.411	5127.519	3203.247
b_0	3.538275607	3.456913	3.401834	3.313691	3.366954	3.396787	3.412314
b_1	-1.193880007	-1.29963	-1.17265	-1.40136	-1.66758	-1.91594	-2.53053
b_2	2.963635512	1.958413	2.175444	1.06635	0.491436	0.572978	1.406665
b_3	11.05454828	13.03508	8.257983	10.4294	9.786554	9.239158	5.313174
b_4	5.005472414	7.689361	2.504236	8.926974	8.991102	6.5447	0.489121
b_5	-56.65820529	-65.8449	-40.8437	-51.3569	-43.7961	-35.5784	-12.8829
c_0	-0.247286226	-0.28301	-0.34424	-0.44452	-0.60198	-0.66077	-0.67352
c_1	-0.038155312	0.007216	0.008923	0.07413	0.183635	0.324023	0.685322
c_2	-0.307554498	-0.2229	-0.27936	0.006675	0.229218	0.154758	-0.11715
c_3	1.289711129	0.366444	0.450635	-0.46446	-1.47713	-2.27586	-1.87656
c_4	0.98591878	0.605957	1.135599	-0.88035	-1.92964	-1.70993	-0.414
c_5	-4.746214526	-0.36417	-0.83384	3.573972	8.028263	8.998669	4.618254
T_0	980	K					
p_0	9.00E+06	Pa					
p, T_u, s_L in Pa, K, and cm/s respectively							

Table 3. Laminar flame speed correlation coefficients for lean to rich conditions.

Ultra-lean mixtures $0.4 \leq \Phi < 0.7$							
		NH100	NH80	NH60	NH40	NH20	NH10	NH0
PSF	l_3	5.972257	8.280904	8.773958	7.502022	5.924598	4.401368	3.102385
	l_2	-0.6229711	-1.28478	-1.67578	-1.49147	-0.76252	0.003777	1.249869
	l_1	-2.552509	-2.48575	-2.42125	-2.43415	-2.60829	-2.75156	-3.10847
	l_0	0.9090909	0.909091	0.909091	0.909091	0.909091	0.909091	0.909091
	m_2	0.5666433	0.562997	0.553841	0.585172	0.583881	0.487537	0.47124

TSF	m_2^{low}	-5.155355	-7.02691	-9.50077	-6.55194	-5.70313	-4.45211	-3.15498
	m_1^{low}	4.963472	6.299628	8.924876	5.913606	5.141422	3.978377	2.699344
	m_0^{low}	-0.8604738	-0.98848	-1.65537	-0.98543	-0.86103	-0.63238	-0.35781
	q_2^{low}	10.42461	13.27763	16.39032	13.02499	11.29109	9.265974	8.091815
	q_1^{low}	-7.991979	-10.3278	-13.5988	-10.016	-8.218	-6.24191	-5.06846
	q_0^{low}	1.411804	1.793722	2.617413	1.765164	1.341947	0.901222	0.623312
	m_2^{med}	-11.5729	-5.83254	-9.40161	-6.66646	-2.35584	-3.29345	-2.27434
	m_1^{med}	10.86622	4.871959	8.478744	5.638625	1.430329	2.616936	1.740849
	m_0^{med}	-2.099847	-0.6036	-1.45213	-0.79119	0.150683	-0.24983	-0.11069
	q_2^{med}	18.92678	12.0076	16.47603	12.40144	6.253099	7.20046	6.397995
	q_1^{med}	-15.74077	-8.58876	-13.0894	-8.74472	-2.63123	-3.87281	-3.24678
	q_0^{med}	3.008928	1.257445	2.312846	1.247228	-0.17654	0.253861	0.164912
	m_2^{med}	-7.669285	-3.65133	-2.92947	-9.25431	-4.26307	-0.56374	-1.73764
	m_1^{high}	7.027129	2.452015	1.985892	8.264429	3.255328	-0.28415	1.104162
	m_0^{high}	-1.238577	-0.03534	-0.00134	-1.41972	-0.2805	0.490161	0.039086
	q_2^{high}	13.43263	8.508435	7.293745	14.96952	7.968012	2.845925	5.176358
	q_1^{high}	-10.24238	-4.59959	-3.7127	-11.2472	-4.18835	0.716587	-1.87654
	q_0^{high}	1.744985	0.269723	0.156335	1.813627	0.182378	-0.89711	-0.1449
	T_{ref}	720	K					
	p_{ref}	9.00E+06	Pa					
	w_T	5						
	w_p	1						

s_L (Φ=0.7, T_u) laminar flame speed in cm/s at Φ =0.7

p, T_u, s_L in Pa, K, and cm/s respectively

Table 4. Laminar flame speed correlation coefficients for ultra-lean conditions.

Am	Aq	am	aq
-0.019788	0.0404458	0.9534167	2.622453

Table 5. Scaling and exponential factor values for the generalized correlation.

In all the equations above, S.I. units are used except for the predicted values of laminar flame speeds, which are in cm/s.

In the first part of this study, seven correlations are derived, one for each NH_3/H_2 blend, including the options of pure NH_3 and pure H_2. For each blend and physical/chemical state, a relative measure of the difference between the value predicted using the correlation $s_{L,fit}$ and the one provided by chemical kinetics simulations $s_{L,data}$ (i.e. a percentual error) is reckoned as $err\% = (s_{L,fit} - s_{L,data})/s_{L,data}$. Results are summarized in **Fig. 5** using error maps: despite a few isolated peaks are visible, the average err% is below ±2.5%, whereas the maximum err% lies between 10% (NH100) and 16% (NH10 and NH40), and it affects the extremal pressure-temperature range of the fitting (130 bar and 1208 K). A further assessment of the accuracy of the fitted correlations can be made by comparing them with the chemical kinetics database via global quality estimators such as those reported in **Table 6,** for all the operating conditions examined for each one of the seven fuel mixtures (NH0, NH10, NH20, NH40, NH60, NH80, NH100). Details regarding the points characterized by the maximum prediction error (err%) are stored in Table 6: first the raw values of the laminar flame speed both predicted ($s_{L,fit}$) and from simulations ($s_{L,data}$) are reported along with the absolute error $s_{L,fit} - s_{L,data}$, all expressed in cm/s. The overall average err% is lower than 2.5% for the dedicated correlations.

	NH100	NH80	NH60	NH40	NH20	NH10	NH0
Mean err%	1.7%	1.9%	2.3%	2.3%	2.5%	2.2%	1.5%
Number of err% above 5%	44	55	67	59	70	63	54
Maximum err%	10%	15%	12%	16%	13%	16%	15%
$s_{L,fit}$ in cm/s at maximum err%	52.7	19.5	170	89	157	135	194
$s_{L,data}$ in cm/s at maximum err%	58.5	22.9	194	105	181	161	227
$(s_{L,fit} - s_{L,data})$ in cm/s	~ 5.8	~ 3.4	~ 24	~ 16	~ 24	~ 26	~ 33

Table 6. Statistics about the prediction accuracy compared to the chemical kinetics simulation database. The number of predicted values with a percentual error above 5% is the number of values over the 360 total values for each blend.

(Dedicated fitting procedure) NH_3 100mol% (Dedicated fitting procedure) H_2 100mol%

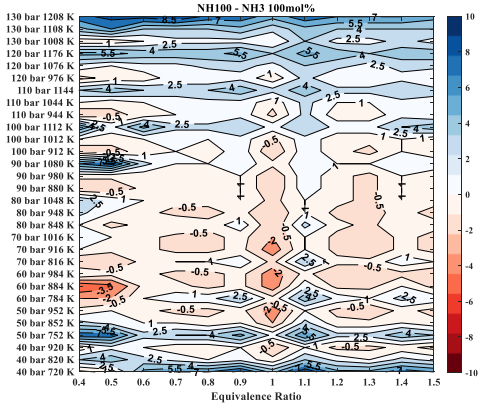

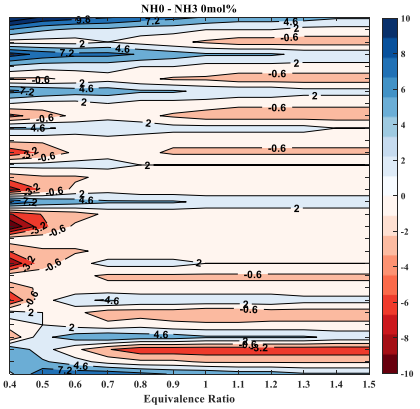

(a)

(Dedicated fitting procedure) NH_3 80mol% - H_2 20mol%

(Dedicated fitting procedure) NH_3 60mol% - H_2 40mol%

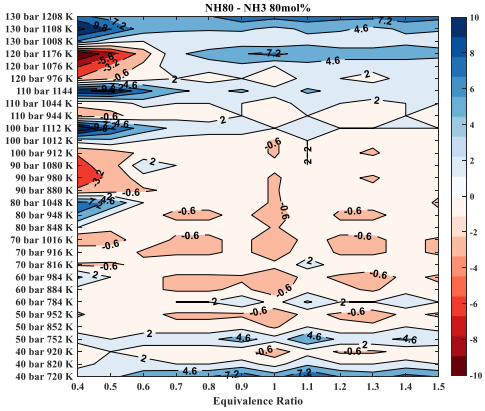

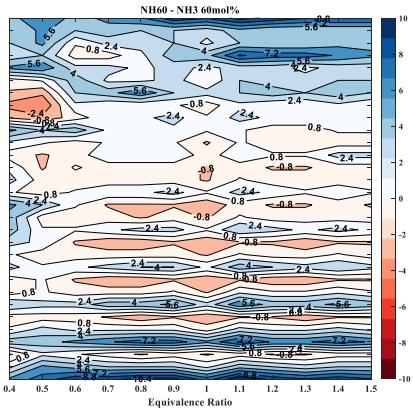

(b)

(Dedicated fitting procedure) NH_3 40mol% - H_2 60mol%

(General fitting procedure) NH_3 40mol% - H_2 60mol%

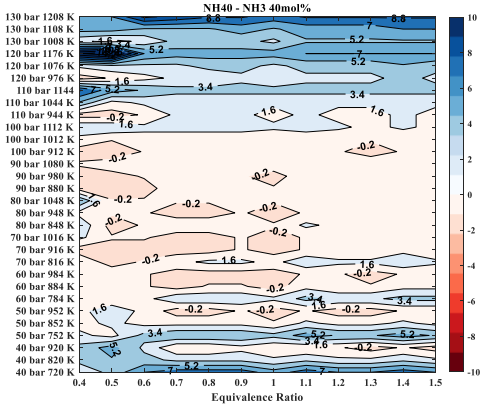

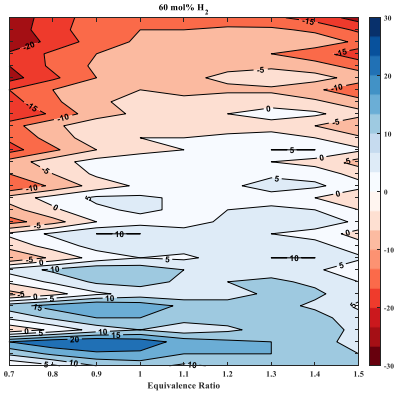

(c)

(Dedicated fitting procedure) NH_3 20mol% - H_2 80mol%

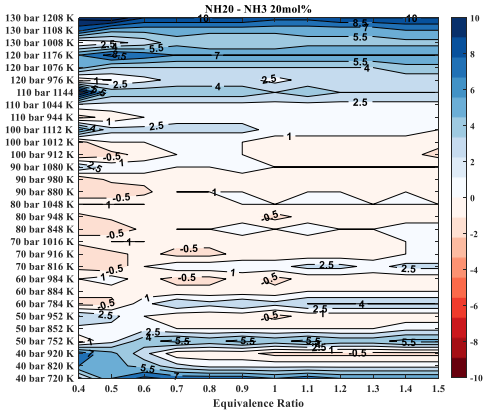

(General fitting procedure) NH_3 20mol% - H_2 80mol%

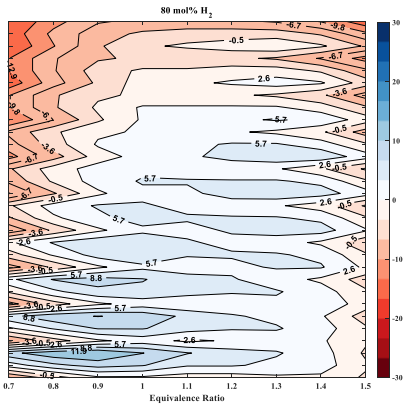

(d)

(Dedicated fitting procedure) NH_3 10mol% - H_2 90mol%

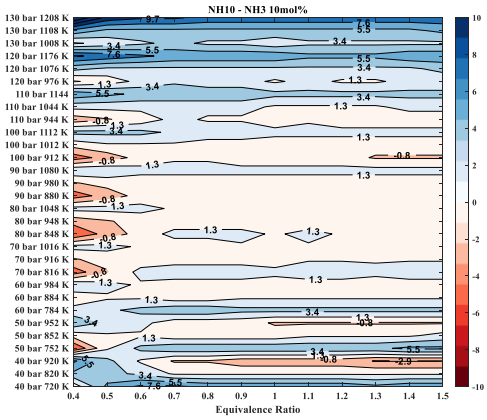

(General fitting procedure) NH_3 10mol% - H_2 90mol%

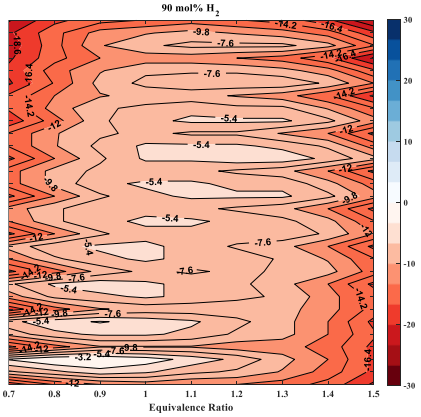

(e)

Figure 5. Error map with relative error.

As for the generalized correlation, the error increases slightly. Despite the lower accuracy, it is worth reminding that a generalized correlation can be useful in the conceptual design stage of the combustion system where the detailed characteristics of the fuel are yet to be determined and they can be used as a degree of freedom in the design space. In cases where a wide range of solutions and conditions have to be tested, a reasonably accurate estimate of the effect of different H_2 content can be quickly provided relying on the sole availability of the laminar burning velocity of pure H_2. Moreover, since the generalized correlation is derived by scaling the H_2 correlation, in this case the estimated err% inherits

the err% from the H_2 correlation (average mean err% equal to 1.51%). The reason for this strategy of evaluation of err% stems from the CFD combustion modelling workflow, in which correlations are provided as polynomial expressions.

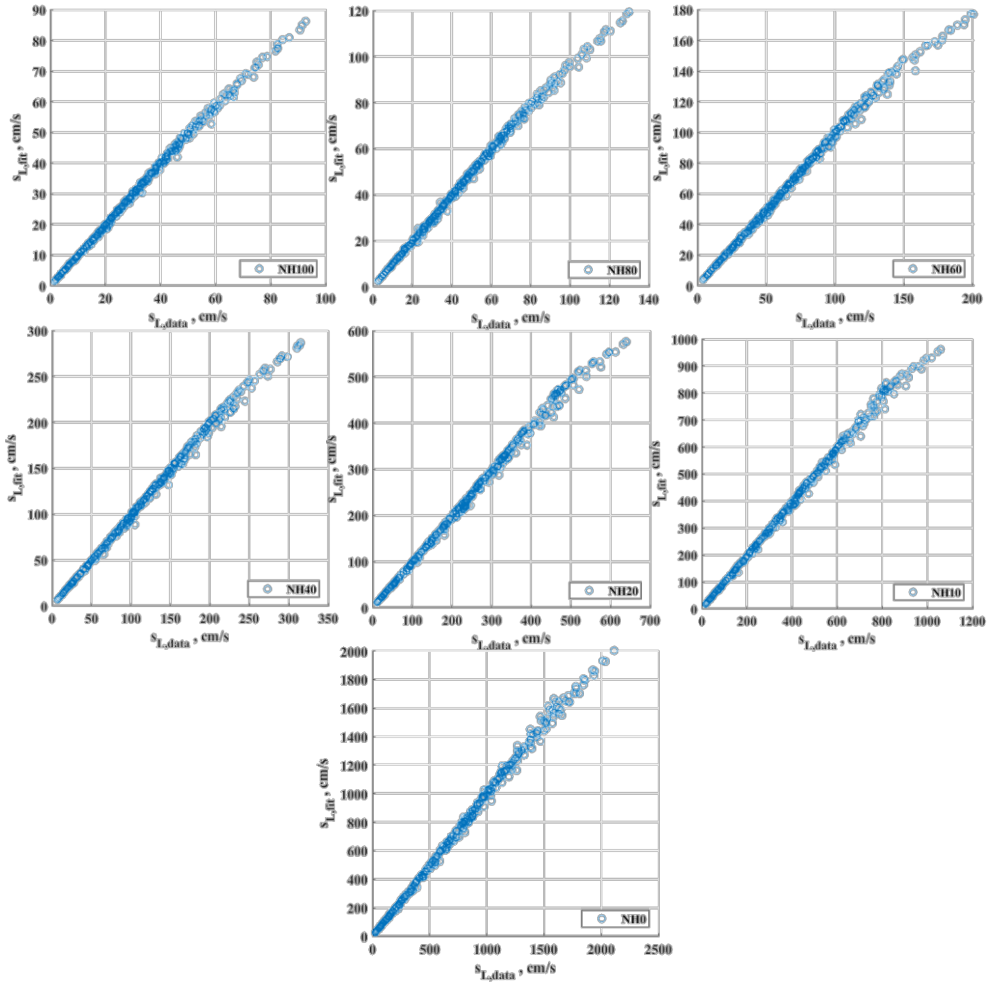

Figure 6. Correlation study comparing dedicated fitting values with the database ones from chemical kinetics simulations.

An additional test to evaluate the proposed correlations is performed through the comparison against those available in literature, compared to Goldmann's [42] and to Verhelst's [40] respectively. For the sake of compactness, only the cases with NH100 and NH0 are considered. Since the correlations proposed by Verhelst [40] for H_2 is valid within a reduced pressure range, the evaluation of the laminar

flame speed is firstly carried out within the validity range. Nevertheless, since a need to apply the correlation for higher pressure may rise for typical ICE full-load conditions, the comparison is then extended beyond such range to help readers to understand the validity of the proposed method [40]. **Fig. 7** and **Fig. 8** show that, while results at low pressures and temperatures confirm the validity of the correlations in literature, outside the validity range the correlations start to largely deviate from the chemical kinetics outcomes. In particular, Goldmann provides unrealistic values for ultra-lean NH_3/air mixtures (values of $\Phi \leq 0.5$ out of the fitting range [42]), while Verhelst provides excessively low laminar flame speed values for very high pressures (beyond the validity range). For this reason, the use of those correlations [42] outside their validity range is questionable at full-load engine-like conditions, motivating the alternative choice provided in the present study.

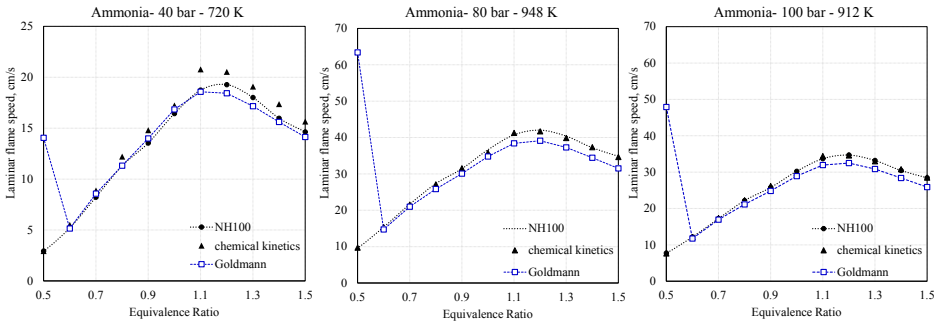

Figure 7. Laminar flame speed prediction at high pressures and temperatures for NH_3/air mixtures.

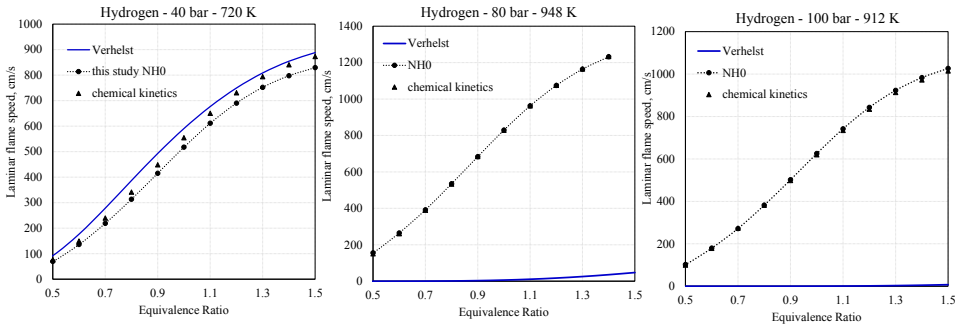

Figure 8. Laminar flame speed prediction at high pressures and temperatures for H_2 /air mixtures.

Finally, values of laminar flame speed for the NH_3/H_2 mixtures obtained with the fitting procedure are depicted in **Fig. 9**: the increment of laminar burning velocity is coherent with the addition of H_2 in the

mixture, as expected. Moreover, a comparison with the laminar flame speeds for a gasoline surrogate E5 (with 5% of oxygenated compounds) from [37] is proposed in **Fig. 9**(a) as an example of the potential differences between a conventional gasoline and an alternative NH_3/H_2 blend in terms of laminar flame speed. The effect of the pressure and temperature is also evaluated for the NH_3/H_2 and the E5 surrogate: by fixing the temperature (948 K) first (**Fig. 9**(b)), and secondly (**Fig. 9**(c)), stark differences occur only for H_2 content above 80 mol%. Coherent increase of laminar flame speed with the higher temperatures at fixed pressure (**Fig. 9**(c)), whereas a decrease of the laminar flame speed is spotted when the pressure is increased at fixed temperature (**Fig. 9**(b)) since the flame front is expected to be thinner as the pressure increases.

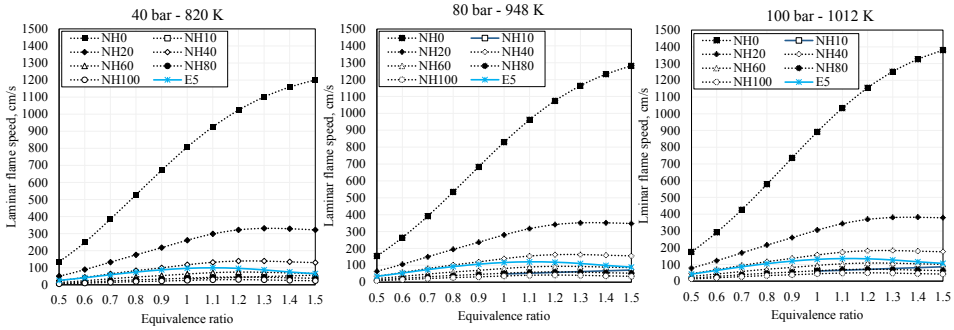

(a)

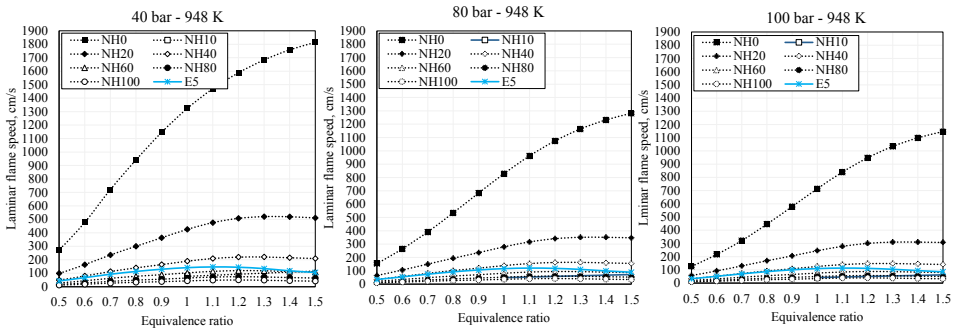

(b)

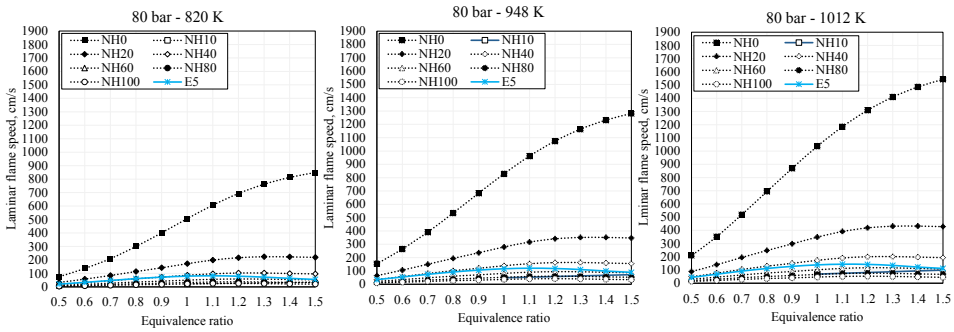

(c)

Figure 9. Laminar flame speed values for NH_3/H_2 blends (NH0-10-20-40-60-80-100) and for a gasoline surrogate as an example of conventional fuels for spark ignition engines(E5).

Finally, a further comparison for different x_{H_2} is carried out between this study blend-specific correlations and the one provided by literature [42]. For a test point (800 K and 45 bar) the laminar flame speed increment with the increase of x_{H_2} is caught in accordance with the values obtained with the correlation provided by Goldamann et al. with similar values (**Fig.10**).

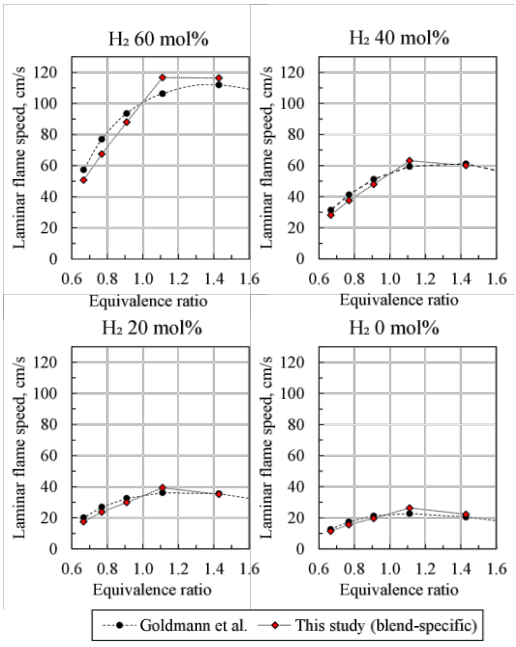

Figure 10. Laminar flame speed increment with increase of x_{H_2} : comparison of values obtained using the correlation by Goldmann and the blend-specific correlation developed in this study.

4. Conclusions

In this study, correlations providing laminar flame speed values are derived using a dedicated fitting procedure over chemical kinetics simulation data (over 2500 total values, 360 for each blend). A dataset of values of freely propagating laminar flames was calculated from 1D chemical kinetics simulations for H_2 /air (NH0), NH_3/air (NH100) and NH_3/H_2 /air mixtures with an increasing H_2 content (10-20-40-60-80 mol%). The applied fitting procedure produces an average prediction error that is ~ 2.5% or lower for each of the seven blends investigated in this study, whereas the maximum err%, which lies between 10% (NH100) and 16% (NH10 and NH40) is usually spotted for the extremal pressure-temperature condition (e.g. 130 bar and 1208 K). The correlation validity range is suitable for full-load conditions in SI engines, i.e., for pressure ranging from 40 bar to 130 bar, unburnt temperatures from 720 K to 1208 K, and ultra-lean (from $\Phi = 0.4$) to rich mixtures (up to $\Phi = 1.5$). Thus, these correlations provide an alternative to the existing ones, whose application outside the validity range result in non-negligible errors. As for the fitting methodology, a simple polynomial correlation is employed for prediction within the range of $0.7 \leq \Phi \leq 1.5$, whereas a dedicated scaling procedure is employed to target the ultra-lean branch of the laminar flame speed. Finally, an attempt to derive a generalized correlation for high H_2 content (from 60mol% up to 90mol%) is presented for lean-to-rich mixtures ($0.7 \leq \Phi \leq 1.5$). Despite the percentual error is lower than 10%, the generalized correlation is less accurate than the dedicated fittings. The proposed correlations play a key role in flamelet combustion models, and they can be easily implemented in any CFD code.

Acknowledgments

Prof. Mehl and the POLIMI unit would like to acknowledge Mario Messina, Lorenzo Mingoia, Michele Nosari, Francesca Trivisonne and Giuseppe Nava, B.Sc. students at POLIMI, for contributing to the kinetic calculations used to formulate the correlations discussed in the paper.

The authors gratefully acknowledge the FAR 2021 for co-funding the project.

Symbols and abbreviations

Abbreviations	
CO	Carbon Monoxide
CO_2	Carbon Dioxide
NO_x	Nitrogen Oxides
CFD	Computational Fluid Dynamics
NH_3	Ammonia
H_2	Hydrogen
ICEs	Internal Combustion Engines
CH_4	methane
SI	Spark Ignition
NH100	blend with NH_3 100 mol%
NH80	blend with NH_3 80 mol%
NH60	blend with NH_3 60 mol%
NH40	blend with NH_3 40 mol%
NH20	blend with NH_3 20 mol%
NH10	blend with NH_3 10 mol%
NH0	blend with NH_3 0 mol%
C_8H_{18}	iso-octane
E5	European Gasoline Surrogate
1D	one-dimensional
3D	three-dimensional
CFD	Computational Fluid Dynamics

Symbols	
Φ	Equivalence ratio
λ	Air index $\lambda = \Phi^{-1}$
p	pressure
mol%	Mole fraction percentage
T_u	Unburnt temperature
s_L	Laminar flame speed
T_0	Reference temperature for lean-to-rich correlation
p_0	Reference pressure for lean-to-rich correlation
$\Phi\|_{0.7}$	Equivalence ratio equal to 0.7
PSF	Pressure scaling factor
TSF	Temperature scaling factor
w_p	Pressure weight
w_T	Temperature weight
T_{ref}	Reference temperature for ultra-lean mixtures
p_{ref}	Reference pressure for ultra-lean mixtures
$s_{L,mix}$	Laminar flame speed for ammonia/H_2 mixture with generalized correlation
x_{H_2}	H_2 mole fraction
$\bar{\Phi}$	Specific value of equivalence ratio
s_{L,H_2}	H_2 laminar flame speed
$s_{L,fit}$	Predicted laminar flame speed
$s_{L,data}$	Laminar flame speed data form chemical kinetics
err%	Prediction percentual error

References

[1] "International Energy Outlook 2016," p. 290, 2016.

[2] H. Xiao, A. Valera-Medina, and P. J. Bowen, "Modeling Combustion of Ammonia/Hydrogen Fuel Blends under Gas Turbine Conditions," *Energy Fuels*, vol. 31, no. 8, pp. 8631–8642, Aug. 2017, doi: 10.1021/acs.energyfuels.7b00709.

[3] A. Valera-Medina *et al.*, “Review on Ammonia as a Potential Fuel: From Synthesis to Economics,” *Energy Fuels*, vol. 35, no. 9, pp. 6964–7029, May 2021, doi: 10.1021/acs.energyfuels.0c03685.
[4] J. S. Cardoso, V. Silva, R. C. Rocha, M. J. Hall, M. Costa, and D. Eusébio, “Ammonia as an energy vector: Current and future prospects for low-carbon fuel applications in internal combustion engines,” *Journal of Cleaner Production*, vol. 296, p. 126562, May 2021, doi: 10.1016/j.jclepro.2021.126562.
[5] A. M. Elbaz, S. Wang, T. F. Guiberti, and W. L. Roberts, “Review on the recent advances on ammonia combustion from the fundamentals to the applications,” *Fuel Communications*, vol. 10, p. 100053, Mar. 2022, doi: 10.1016/j.jfueco.2022.100053.
[6] P. Kumar and T. R. Meyer, “Experimental and modeling study of chemical-kinetics mechanisms for H2–NH3–air mixtures in laminar premixed jet flames,” *Fuel*, vol. 108, pp. 166–176, Jun. 2013, doi: 10.1016/j.fuel.2012.06.103.
[7] J. H. Lee, J. H. Kim, J. H. Park, and O. C. Kwon, “Studies on properties of laminar premixed hydrogen-added ammonia/air flames for hydrogen production,” *International Journal of Hydrogen Energy*, vol. 35, no. 3, pp. 1054–1064, Feb. 2010, doi: 10.1016/j.ijhydene.2009.11.071.
[8] A. Karan, G. Dayma, C. Chauveau, and F. Halter, “High-pressure and temperature ammonia flame speeds,” p. 6.
[9] A. Hayakawa, Y. Arakawa, R. Mimoto, K. D. K. A. Somarathne, T. Kudo, and H. Kobayashi, “Experimental investigation of stabilization and emission characteristics of ammonia/air premixed flames in a swirl combustor,” *International Journal of Hydrogen Energy*, vol. 42, no. 19, pp. 14010–14018, May 2017, doi: 10.1016/j.ijhydene.2017.01.046.
[10] Mashruk Syed, Kovaleva Marina, Chong Cheng Tung, Hayakawa Akihiro, Okafor Ekenechukwu, and Valera-Medina Agustin, “Nitrogen Oxides as a By-product of Ammonia/Hydrogen Combustion Regimes,” *Chemical Engineering Transactions*, vol. 89, pp. 613–618, Dec. 2021, doi: 10.3303/CET2189103.
[11] E. C. Okafor *et al.*, “Influence of wall heat loss on the emission characteristics of premixed ammonia-air swirling flames interacting with the combustor wall,” *Proceedings of the Combustion Institute*, vol. 38, no. 4, pp. 5139–5146, 2021, doi: 10.1016/j.proci.2020.06.142.
[12] H. Xiao, M. S. Howard, A. Valera-Medina, S. Dooley, and P. Bowen, “Reduced Chemical Mechanisms for Ammonia/Methane Co-firing for Gas Turbine Applications,” *Energy Procedia*, vol. 105, pp. 1483–1488, May 2017, doi: 10.1016/j.egypro.2017.03.441.
[13] M.-C. Chiong *et al.*, “Advancements of combustion technologies in the ammonia-fuelled engines,” *Energy Conversion and Management*, vol. 244, p. 114460, Sep. 2021, doi: 10.1016/j.enconman.2021.114460.
[14] K. P. Shrestha *et al.*, “An experimental and modeling study of ammonia with enriched oxygen content and ammonia/hydrogen laminar flame speed at elevated pressure and temperature,” *Proceedings of the Combustion Institute*, vol. 38, no. 2, pp. 2163–2174, 2021, doi: 10.1016/j.proci.2020.06.197.
[15] A. A. Khateeb *et al.*, “Stability limits and NO emissions of premixed swirl ammonia-air flames enriched with hydrogen or methane at elevated pressures,” *International Journal of Hydrogen Energy*, vol. 46, no. 21, pp. 11969–11981, Mar. 2021, doi: 10.1016/j.ijhydene.2021.01.036.
[16] C. Lhuillier, P. Brequigny, F. Contino, and C. Mounaïm-Rousselle, “Experimental study on ammonia/hydrogen/air combustion in spark ignition engine conditions,” *Fuel*, vol. 269, p. 117448, Jun. 2020, doi: 10.1016/j.fuel.2020.117448.
[17] S. Verhelst and T. Wallner, “Hydrogen-fueled internal combustion engines,” *Progress in Energy and Combustion Science*, vol. 35, no. 6, pp. 490–527, Dec. 2009, doi: 10.1016/j.pecs.2009.08.001.
[18] S. B. Pope, “Turbulent Premixed Flames,” *Annu. Rev. Fluid Mech.*, vol. 19, no. 1, pp. 237–270, Jan. 1987, doi: 10.1146/annurev.fl.19.010187.001321.
[19] N. Peters, *Turbulent Combustion*. Cambridge University Press, 2000.
[20] T. Poinsot and D. Veynante, *Theoretical and Numerical Combustion*. Edwards, 2005.
[21] E. Ranzi *et al.*, “Hierarchical and comparative kinetic modeling of laminar flame speeds of hydrocarbon and oxygenated fuels,” *Progress in Energy and Combustion Science*, vol. 38, no. 4, pp. 468–501, Aug. 2012, doi: 10.1016/j.pecs.2012.03.004.

[22] J. M. Boyde, A. Fiolitakis, M. Di Domenico, and M. Aigner, “Correlations for the Laminar Flame Speed, Adiabatic Flame Temperature and Ignition Delay Time for Methane, Ethanol and n-Decane,” in *49th AIAA Aerospace Sciences Meeting including the New Horizons Forum and Aerospace Exposition*, 0 vols., American Institute of Aeronautics and Astronautics, 2011. doi: 10.2514/6.2011-510.

[23] M. Metghalchi and J. C. Keck, “Laminar burning velocity of propane-air mixtures at high temperature and pressure,” *Combustion and Flame*, vol. 38, pp. 143–154, Jan. 1980, doi: 10.1016/0010-2180(80)90046-2.

[24] R. Amirante, E. Distaso, P. Tamburrano, and R. D. Reitz, “Laminar flame speed correlations for methane, ethane, propane and their mixtures, and natural gas and gasoline for spark-ignition engine simulations,” *International Journal of Engine Research*, vol. 18, no. 9, pp. 951–970, Nov. 2017, doi: 10.1177/1468087417720018.

[25] N. Wang *et al.*, “Laminar burning characteristics of ammonia/hydrogen/air mixtures with laser ignition,” *International Journal of Hydrogen Energy*, vol. 46, no. 62, pp. 31879–31893, Sep. 2021, doi: 10.1016/j.ijhydene.2021.07.063.

[26] S. Wang, A. M. Elbaz, Z. Wang, and W. L. Roberts, “The effect of oxygen content on the turbulent flame speed of ammonia/oxygen/nitrogen expanding flames under elevated pressures,” *Combustion and Flame*, vol. 232, p. 111521, Oct. 2021, doi: 10.1016/j.combustflame.2021.111521.

[27] A. Ichikawa, A. Hayakawa, Y. Kitagawa, K. D. Kunkuma Amila Somarathne, T. Kudo, and H. Kobayashi, “Laminar burning velocity and Markstein length of ammonia/hydrogen/air premixed flames at elevated pressures,” *International Journal of Hydrogen Energy*, vol. 40, no. 30, pp. 9570–9578, Aug. 2015, doi: 10.1016/j.ijhydene.2015.04.024.

[28] R. Kanoshima *et al.*, “Effects of initial mixture temperature and pressure on laminar burning velocity and Markstein length of ammonia/air premixed laminar flames,” *Fuel*, vol. 310, p. 122149, Feb. 2022, doi: 10.1016/j.fuel.2021.122149.

[29] M. Mitu, D. Razus, and V. Schroeder, “Laminar Burning Velocities of Hydrogen-Blended Methane–Air and Natural Gas–Air Mixtures, Calculated from the Early Stage of p(t) Records in a Spherical Vessel,” *Energies*, vol. 14, no. 22, p. 7556, Nov. 2021, doi: 10.3390/en14227556.

[30] G. J. Gotama *et al.*, “Measurement of the laminar burning velocity and kinetics study of the importance of the hydrogen recovery mechanism of ammonia/hydrogen/air premixed flames,” *Combustion and Flame*, vol. 236, p. 111753, Feb. 2022, doi: 10.1016/j.combustflame.2021.111753.

[31] X. Han, Z. Wang, M. Costa, Z. Sun, Y. He, and K. Cen, “Experimental and kinetic modeling study of laminar burning velocities of NH3/air, NH3/H2/air, NH3/CO/air and NH3/CH4/air premixed flames,” *Combustion and Flame*, vol. 206, pp. 214–226, Aug. 2019, doi: 10.1016/j.combustflame.2019.05.003.

[32] E. C. Okafor *et al.*, “Experimental and numerical study of the laminar burning velocity of CH4–NH3–air premixed flames,” *Combustion and Flame*, vol. 187, pp. 185–198, Jan. 2018, doi: 10.1016/j.combustflame.2017.09.002.

[33] J. Otomo, M. Koshi, T. Mitsumori, H. Iwasaki, and K. Yamada, “Chemical kinetic modeling of ammonia oxidation with improved reaction mechanism for ammonia/air and ammonia/hydrogen/air combustion,” *International Journal of Hydrogen Energy*, vol. 43, no. 5, pp. 3004–3014, Feb. 2018, doi: 10.1016/j.ijhydene.2017.12.066.

[34] Y. Song *et al.*, “The sensitizing effects of NO2 and NO on methane low temperature oxidation in a jet stirred reactor,” *Proceedings of the Combustion Institute*, vol. 37, no. 1, pp. 667–675, 2019, doi: 10.1016/j.proci.2018.06.115.

[35] A. Stagni *et al.*, “An experimental, theoretical and kinetic-modeling study of the gas-phase oxidation of ammonia,” *React. Chem. Eng.*, vol. 5, no. 4, pp. 696–711, 2020, doi: 10.1039/C9RE00429G.

[36] M. Del Pecchia, S. Breda, A. D’Adamo, S. Fontanesi, A. Irimescu, and S. Merola, “Development of Chemistry-Based Laminar Flame Speed Correlation for Part-Load SI Conditions and Validation in a GDI Research Engine,” *SAE Int. J. Engines*, vol. 11, no. 6, pp. 715–741, Apr. 2018, doi: 10.4271/2018-01-0174.

[37] M. Del Pecchia, V. Pessina, F. Berni, A. d'Adamo, and S. Fontanesi, "Gasoline-ethanol blend formulation to mimic laminar flame speed and auto-ignition quality in automotive engines," *Fuel*, vol. 264, p. 116741, Mar. 2020, doi: 10.1016/j.fuel.2019.116741.

[38] M. Di Lorenzo, P. Brequigny, F. Foucher, and C. Mounaïm-Rousselle, "Validation of TRF-E as gasoline surrogate through an experimental laminar burning speed investigation," *Fuel*, vol. 253, pp. 1578–1588, Oct. 2019, doi: 10.1016/j.fuel.2019.05.081.

[39] S. Verhelst, R. Woolley, M. Lawes, and R. Sierens, "Laminar and unstable burning velocities and Markstein lengths of hydrogen–air mixtures at engine-like conditions," *Proceedings of the Combustion Institute*, vol. 30, no. 1, pp. 209–216, Jan. 2005, doi: 10.1016/j.proci.2004.07.042.

[40] S. Verhelst, C. T'Joen, J. Vancoillie, and J. Demuynck, "A correlation for the laminar burning velocity for use in hydrogen spark ignition engine simulation," *International Journal of Hydrogen Energy*, vol. 36, no. 1, pp. 957–974, Jan. 2011, doi: 10.1016/j.ijhydene.2010.10.020.

[41] G. D'Errico, A. Onorati, and S. Ellgas, "1D thermo-fluid dynamic modelling of an S.I. single-cylinder H2 engine with cryogenic port injection," *International Journal of Hydrogen Energy*, vol. 33, no. 20, pp. 5829–5841, Oct. 2008, doi: 10.1016/j.ijhydene.2008.05.096.

[42] A. Goldmann and F. Dinkelacker, "Approximation of laminar flame characteristics on premixed ammonia/hydrogen/nitrogen/air mixtures at elevated temperatures and pressures," *Fuel*, vol. 224, pp. 366–378, Jul. 2018, doi: 10.1016/j.fuel.2018.03.030.

[43] S. Brusca, R. Lanzafame, A. M. C. Garrano, and M. Messina, "Effects of Pressure, Temperature and Dilution on Fuels/Air Mixture Laminar Flame Burning Velocity," *Energy Procedia*, vol. 82, pp. 125–132, Dec. 2015, doi: 10.1016/j.egypro.2015.12.004.

[44] V. Di Sarli and A. D. Benedetto, "Laminar burning velocity of hydrogen–methane/air premixed flames," *International Journal of Hydrogen Energy*, vol. 32, no. 5, pp. 637–646, Apr. 2007, doi: 10.1016/j.ijhydene.2006.05.016.

[45] E. Ranzi, A. Frassoldati, A. Stagni, M. Pelucchi, A. Cuoci, and T. Faravelli, "Reduced Kinetic Schemes of Complex Reaction Systems: Fossil and Biomass-Derived Transportation Fuels: REDUCED KINETIC SCHEMES OF COMPLEX REACTION SYSTEMS," *Int. J. Chem. Kinet.*, vol. 46, no. 9, pp. 512–542, Sep. 2014, doi: 10.1002/kin.20867.

[46] A. Stagni, A. Cuoci, A. Frassoldati, T. Faravelli, and E. Ranzi, "Lumping and Reduction of Detailed Kinetic Schemes: an Effective Coupling," *Ind. Eng. Chem. Res.*, vol. 53, no. 22, pp. 9004–9016, Jun. 2014, doi: 10.1021/ie403272f.

[47] A. Stagni, A. Frassoldati, A. Cuoci, T. Faravelli, and E. Ranzi, "Skeletal mechanism reduction through species-targeted sensitivity analysis," *Combustion and Flame*, vol. 163, pp. 382–393, Jan. 2016, doi: 10.1016/j.combustflame.2015.10.013.